Hindawi
Mathematical Problems in Engineering
Volume 2019, Article ID 1019621, 10 pages
https://doi.org/10.1155/2019/1019621

*Research Article*

# Adaptive Backstepping Control for Longitudinal Dynamics of Hypersonic Vehicle Subject to Actuator Saturation and Disturbance

**Zhiqiang Jia**,[1,2] **Tianya Li**,[2] **and Kunfeng Lu**[2]

[1] *The School of Automation, Beijing Institute of Technology, Beijing, China*
[2] *Beijing Aerospace Automatic Control Institute, Beijing, China*

Correspondence should be addressed to Zhiqiang Jia; chrisjia82@163.com

Received 8 November 2018; Revised 27 December 2018; Accepted 17 January 2019; Published 3 March 2019

Academic Editor: Andrzej Swierniak



In this paper, an adaptive backstepping control strategy is presented to solve the longitudinal control problem for a hypersonic vehicle (HSV) subject to actuator saturation and disturbances. Small perturbation linearization transforms the dynamics to a seconded-order system at each trimming point, with total disturbance including unmodeled dynamics, parametric uncertainties, and external disturbances. The disturbance can be estimated and compensated for by an extended state observer (ESO), and thus the system is decoupled. To deal with the actuator saturation and wide flight envelope, an adaptive backstepping control strategy is designed. A rigorous proof of finite-time convergence is provided applying Lyapunov method. The effectiveness of the proposed control scheme is verified in simulations.

## 1. Introduction

Attitude control is a typical nonlinear control problem, which is very important for spacecraft, missile, HSV, and so on in engineering practice. According to small perturbation assumption, the flight dynamics of HSVs can be linearized around the trimming points. Then, the classical control methods such as PID and feedback linearization are employed to design the controller [1–3]. Hypersonic vehicle is required to work within a large flight envelope to meet the challenge of highly maneuverable targets in all probable engagements [4]. Due to the wide envelope, a great number of operating points should be carefully chosen to cover the full envelop, and an effective controller should be designed for each point. Note that the designed control algorithms should guarantee stability with superior control performance and robustness throughout the flight envelope [5, 6]. However, the equations of motion that govern the behavior of an HSV are nonlinear and time varying, which make flight control system design for aircraft a complex and difficult problem. Considering the uncertainties in aerodynamic parameters, nonlinearities and measurement noises, the task of guaranteeing favorable control performance and robustness throughout the entire flight envelope is a challenging one.

Due to the practical importance of HSV, the attitude control has attracted extensive attention and a great number of control methods have been designed to improve control performance. In [7–10], the backstepping procedure is designed for an angle of attack autopilot. Furthermore, to deal with the explosion of the complexity associated with the backstepping method, improving the dynamic surface control method has been studied in [11] on the longitudinal dynamics of HSV. Although the above literature can obtain some meaningful results on the HSV control, this algorithm has low robustness under the uncertainties. Since sliding mode control (SMC) technique provides robustness to internal parameter variations and extraneous disturbance satisfying the matching condition, addressing the velocity and altitude tracking control of hypersonic vehicle has been introduced in [1, 10, 12, 13]. These designed laws guaranteed that both velocity and altitude track fast their reference trajectories respectively under both uncertainties and external disturbances, and it has been also confirmed by the simulation results. But the above-mentioned SMC methods inherently

suffer from the chattering problem, which is an undesired phenomenon in practice systems. In [14], the $H_\infty$ control with gain scheduling and dynamic inversion (DI) methods is designed for the aircraft. The time-domain and frequency-domain analysis procedures show that these methods possess strong robustness and high control performance. Based on DI methods, the feedback linearization technique is used to design the controller for the attitude control of HSV [15–17], where the nonlinear dynamics of system is converted into a chain of integrators in the design of inner-loop nonlinear control law. Although DI method can obtain some meaningful results on the HSV control, this algorithm is sensitive to the modelling errors [18–22]. Therefore, a model-free framework for the DI strategy is urgently needed.

Based on the feedback linearization approach, Han proposes a novel philosophy, active disturbance rejection control (ADRC), which does not rely on a refined dynamic model [23]. A linear ADRC controller is then presented for practical applications, since the parameter tuning process is simplified [24]. ESO is the core concept of ADRC and has demonstrated its effectiveness in many fields. In [25], an ESO-based control scheme is presented to handle the initial turning problem for a vertical launching air-defense missile. Based on the work of [25], Tian et al. [26] employ ADRC to a generic nonlinear uncertain system with mismatched disturbances, and then a robust output feedback autopilot for an HSV is devised. In [27], a control method combining ADRC and optimal control is discussed for large aircraft landing attitude control under external disturbances. The results show that the ESO technique can guarantee the unknown disturbance and model uncertainties rejection. Actually, actuator saturation affects virtually all practical control systems. It may result in performance degradation and even induce instability. The hypersonic vehicle dynamics is inherently nonlinear, and the number of available results by considering actuator saturation in the design and analysis of hypersonic vehicle dynamics is still limited [13, 28]. In this case, the flight envelope of hypersonic vehicle is narrow and the existing actuator saturation deteriorates the control performance, thus the effective control method should be investigated for HSV.

The paper mainly focuses on the longitudinal control problem of HSVs suffering actuator saturation and disturbances within large envelop. The main contributions of this paper are threefold:

(1) A linear ESO is used to estimate and compensate for the total disturbances of the small-perturbation-linearized longitudinal dynamics of HSV, which consists of unmodeled dynamics, parametric uncertainties, and external disturbances.

(2) An adaptive backstepping control law is designed to deal with the large envelop and actuator saturation problem, and a rigorous proof of stability is provided by employing Lyapunov theory.

(3) The control structure considers the complex aerodynamics and ensures the tracking performance with very little requirement of model information, which is suitable for engineering practices.

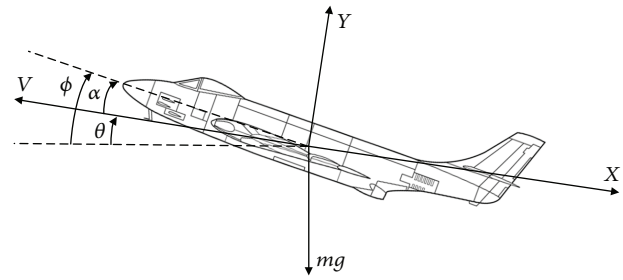


Figure 1: Body diagram of an HSV.

The remainder of this paper is organized as follows: the longitudinal flight model of HSV and problem formulation are presented in the "Preliminaries" section. In the "Control Strategy" section, an ESO-based adaptive backstepping controller is designed, and the closed-loop convergence is analyzed. The "Simulation Results" section gives simulation results and some discussions. Finally, conclusions are drawn in the "Conclusion" section.

## 2. Preliminaries

*2.1. Longitudinal Dynamic Model.* This study is concerned with the longitudinal motion of the vehicle. It is assumed that there is no side slip, no lateral motion, and no roll for the hypersonic vehicle. As shown in Figure 1, the longitudinal dynamic model for a generic HSV is as follows [6]:

$$\begin{aligned} m\frac{\mathrm{d}V}{\mathrm{d}t} &= -X - mg\sin\theta \\ mV\frac{\mathrm{d}\theta}{\mathrm{d}t} &= Y - mg\cos\theta \\ J_z\frac{\mathrm{d}\omega_z}{\mathrm{d}t} &= M_z + M_{gz} \\ \frac{\mathrm{d}\phi}{\mathrm{d}t} &= \omega_z \\ \alpha &= \phi - \theta \end{aligned} \tag{1}$$

where the drag force, lift force, and pitch moment of the HSV are depicted by

$$\begin{aligned} X &= \frac{1}{2}\rho V^2 S C_X\left(\alpha, V, \delta_z\right) \\ Y &= \frac{1}{2}\rho V^2 S C_Y\left(\alpha, V, \delta_z\right) \\ M_z &= \frac{1}{2}\rho V^2 S\bar{c} C_{M_z}\left(\alpha, V, \delta_z\right) \end{aligned} \tag{2}$$

The parameters $\rho$, $S$, and $\bar{c}$ represent the air density, the reference area, and the mean aerodynamic chord, and $C_X$, $C_Y$, and $C_{M_z}$ represent the drag, lift, and moment coefficients, respectively.

Since $X$, $Y$, and $M_z$ are all related to $\delta_z$, the system is strongly coupled. The control objective for this paper is to

find a feedback control $\delta_z$ such that the pitch angle can track the desired trajectory of pitch angle very well. Therefore, we should consider the pitch dynamics and small perturbation method is applied.

Introduce small perturbation assumption, ignore second order or higher order traces and secondary factors of aerodynamic forces and moment, linearize the equations and develop the perturbation equation in three-dimensional space as follows [6]:

$$\begin{aligned}
\frac{d\Delta V}{dt} &= -\frac{X^V}{m}\Delta V - \frac{X^\alpha}{m}\Delta\alpha - g\cos\theta\Delta\theta \\
\frac{d\Delta\theta}{dt} &= \frac{Y^V}{mV}\Delta V + \frac{Y^\alpha}{mV}\Delta\alpha + \frac{g\sin\theta}{V}\Delta\theta + \frac{Y^{\delta_z}}{mV}\Delta\delta_z \\
\frac{d\Delta\omega_z}{dt} &= \frac{M_z^V}{J_z}\Delta V + \frac{M_z^\alpha}{J_z}\Delta\alpha + \frac{M_z^{\omega_z}}{J_z}\Delta\omega_z + \frac{M_z^{\delta_z}}{J_z}\Delta\delta_z \\
&\quad + \frac{M_{gz}}{J_z} \\
\frac{d\Delta\phi}{dt} &= \Delta\omega_z \\
\Delta\alpha &= \Delta\phi - \Delta\theta
\end{aligned} \tag{3}$$

where the aerodynamic coefficient $A^b$ stands for $\partial A/\partial b$ for $A \in \{X, Y, Z\}$ and $b \in \{V, \alpha, \omega_z, \delta_z\}$ and can be obtained from prior knowledge.

Assuming the velocity to be a constant in a short time, then (3) can be simplified as follows:

$$\Delta\ddot{\phi} - a_1\Delta\dot{\phi} - a_2\Delta\alpha - a_3\Delta\dot{\alpha} - a_4\Delta\delta_z = \frac{M_{gz}}{J_z} \tag{4}$$

$$\Delta\dot{\theta} - a_5\Delta\theta - a_6\Delta\alpha = a_7\Delta\delta_z \tag{5}$$

$$\Delta\alpha = \Delta\phi - \Delta\theta \tag{6}$$

where $a_1 = M_z^{\omega_z}/J_z$, $a_2 = M_z^\alpha/J_z$, $a_3 = M_z^{\dot{\alpha}}/J_z$, $a_4 = M_z^{\delta_z}/J_z$, $a_5 = (g\sin\theta)/V$, $a_6 = Y^\alpha/mV$, and $a_7 = Y^{\delta_z}/mV$.

Then the second-order dynamics of pitch angle (4) can be rewritten as follows:

$$\ddot{\phi}(t) = f(\cdot) + a_4\sigma(\delta_z)\delta_z(t) \tag{7}$$

with the total disturbance $f(\cdot)$ defined as

$$f(\cdot) = \ddot{\phi}_r + a_1\Delta\dot{\phi} + a_2\Delta\alpha + a_3\Delta\dot{\alpha} - a_4\delta_{z_0} + \frac{M_{gz}}{J_z} \tag{8}$$

with $\phi_r$ the reference pitch angle, and $\delta_{z_0}$ the deflection angle calculated by the nominal system with reference $\phi_r$, which is not required to be known for subsequent controller design.

The function $\sigma(\cdot)$ is the saturation function of deflection angle defined as follows:

$$\sigma(\delta_z) = \begin{cases} 1 & |\delta_z(t)| \leqslant \overline{\delta_z} \\ \dfrac{\overline{\delta_z}}{\delta_z(t)} \cdot \mathrm{Sign}(\delta_z(t)) & |\delta_z(t)| > \overline{\delta_z} \end{cases} \tag{9}$$

where $\overline{\delta_z}$ is the maximum allowable value of the deflection. Obviously, $\sigma \in (0, 1]$.

Then an assumption for the disturbance is given as follows.

*Assumption 1.* The additive disturbances moment $M_{gz}$ is differentiable, and the derivative is bounded.

*Remark 2.* As shown in (8), the total disturbance $f(\cdot)$ contains coupling terms and external disturbances. According to Assumption 1, $f(\cdot)$ is physically differentiable, which is necessary for further discussion. Applying small perturbation linearization, high-order dynamics and secondary factors are omitted, which brings unmodeled dynamics. Note that the unmodeled dynamics caused by linearization, and the parametric uncertainties can also be concluded in the total disturbance, which is not presented in the equation for simplicity.

*2.2. Extended State Observer.* The ESO is a special state observer estimating both system states and an extended state, which consist of the unknown dynamics and external disturbance of the system. Appropriately designed observers can provide comparatively accurate estimations that can be compensated in the control inputs.

Consider a nonlinear system with uncertainties and external disturbances

$$\begin{aligned}
x^n(t) &= f_1\left(x(t), \dot{x}(t), \ldots, x^{(n-1)}(t)\right) + d_1(t) \\
&\quad + bu(t)
\end{aligned} \tag{10}$$

where $f_1(x(t), \dot{x}(t), \ldots, x^{(n-1)}(t))$ is an unknown function, $d_1(t)$ is the unknown external disturbance, $u(t)$ is the control input, and $b$ is a known constant.

For clarity, System (10) can be rewritten as

$$\begin{aligned}
\dot{x}_1 &= x_2 \\
\dot{x}_2 &= x_3 \\
&\vdots \\
\dot{x}_n &= x_{n+1} + bu \\
\dot{x}_{n+1} &= h(t) \\
y &= x_1
\end{aligned} \tag{11}$$

where

$$x_{n+1} = f_1\left(x(t), \dot{x}(t), \ldots, x^{n-1}(t)\right) + d_1(t) \tag{12}$$

is the extended state.

Then, an ESO can be constructed as follows:

$$\begin{aligned}
\dot{\hat{x}}_1 &= \hat{x}_2 - l_1(\hat{x}_1 - y) \\
&\vdots \\
\dot{\hat{x}}_n &= \hat{x}_{n+1} - l_n(\hat{x}_1 - y) + bu \\
\dot{\hat{x}}_{n+1} &= -l_{n+1}(\hat{x}_1 - y)
\end{aligned} \tag{13}$$

where $\hat{x}_i$ are the observer outputs and $l_i$ are positive observer gains, $i = 1, 2, \ldots, n+1$.

Note that the extended state is the total disturbance, which contains the unknown dynamics and external disturbances. Appropriately designed observers can provide comparatively accurate estimations that can be compensated in the control inputs, which improves the robustness. More detailed description of the principle of ESO can be found in [23].

## 3. Control Strategy

In this section, an ESO-based pitch controller for HSV pitch angle controller is devised. Adaptive backstepping technique is applied with ESO to reject disturbances and unmodeled dynamics. In the first stage, the estimation of total disturbances, including external disturbances and unmodeled dynamics, is discussed. Then, in the second stage, an adaptive backstepping controller is designed, while the estimation of the disturbances is used as a time-varying parameter to improve robustness.

*3.1. Lumped Disturbance Estimation.* In order to improve the robustness, an extended state observer is used to estimate and compensate for the disturbance. Let $x_1 = \phi$, $x_2 = \dot{\phi}$, and regard total disturbance $f(\cdot)$ as an extended state $x_3$, then the longitudinal system in (7) can be expressed as follows:

$$\begin{aligned} \dot{x}_1 &= x_2 \\ \dot{x}_2 &= x_3 + a_4 \sigma(\delta_z)\delta_z \\ \dot{x}_3 &= h(\cdot) \end{aligned} \tag{14}$$

where $h(\cdot) = \dot{f}(\cdot)$ is bounded according to the discussion in Remark 2.

Consider the third-order linear ESO as follows:

$$\begin{aligned} \dot{\hat{x}}_1 &= \hat{x}_2 - 3\omega_o(\hat{x}_1 - x_1) \\ \dot{\hat{x}}_2 &= \hat{x}_3 - 3\omega_o^2(\hat{x}_1 - x_1) + a_4\sigma(\delta_z)\delta_z \\ \dot{\hat{x}}_3 &= -\omega_o^3(\hat{x}_1 - x_1) \end{aligned} \tag{15}$$

where $\hat{x}_1$, $\hat{x}_2$, and $\hat{x}_3$ are the observer outputs and $\omega_o > 0$ is the bandwidth of the ESO. Note that few model information is required for observer design except $a_4$.

It is obvious that the characteristic polynomial is Hurwitz, and the observer is bounded-input-bounded-output (BIBO) stable. Define the estimation error as $\tilde{x}_i = x_i - \hat{x}_i$, $i = 1, 2, 3$, the observer estimation error is as follows:

$$\begin{aligned} \dot{\tilde{x}}_1 &= \tilde{x}_2 - 3\omega_o\tilde{x}_1 \\ \dot{\tilde{x}}_2 &= \tilde{x}_3 - 3\omega_o^2\tilde{x}_1 \\ \dot{\tilde{x}}_3 &= h(\cdot) - \omega_o^3\tilde{x}_1 \end{aligned} \tag{16}$$

Let $\varepsilon_i = \tilde{x}_1/\omega_o^{i-1}$, $i = 1, 2, 3$, and (16) can be simplified as follows:

$$\dot{\varepsilon} = \omega_o A\varepsilon + B\frac{h(\cdot)}{\omega_o^2} \tag{17}$$

where $\varepsilon = [\varepsilon_1 \;\; \varepsilon_2 \;\; \varepsilon_3]^T$, $B = [0 \;\; 0 \;\; 1]^T$ and

$$A = \begin{bmatrix} -3 & 1 & 0 \\ -3 & 0 & 1 \\ -1 & 0 & 0 \end{bmatrix} \tag{18}$$

is Hurwitz.

**Lemma 3** (see [29]). *Assuming $h(\cdot)$ is bounded, there exist a constant $\varrho_i > 0$ and a finite $T_1 > 0$, so that*

$$\begin{aligned} &|\tilde{x}_i(t)| \leqslant \rho_i, \\ &\rho_i = O\left(\frac{1}{\omega_o^{k_1}}\right), \; i = 1, 2, 3, \; \forall t \geqslant T_1 > 0 \end{aligned} \tag{19}$$

*for some positive integer $k_1$, where $O(\cdot)$ represents the infinitely small.*

*Remark 4.* Since $A$ is Hurwitz, error system (17) is BIBO stable. Therefore, the requirement of ESO is the boundedness of $h(\cdot)$. Lemma 3 also indicates a good steady estimation performance of ESO, and the estimation error can be reduced to a sufficient small range within a finite time $T_1$ by increasing the bandwidth $\omega_o$. Since the disturbance $f(\cdot)$ is partly compensated for and the actual disturbance on system becomes $\tilde{x}_i(t)$, the steady control performance is likely to be improved.

With a well-tuned ESO, the total disturbance $f(\cdot)$ can be actively estimated by $\hat{x}_3$. For simplicity, here we denote $\hat{f} = \hat{x}_3$. Since the observer (15) is BIBO stable, the estimation error of $f(\cdot)$ is bounded. Defining $\eta$ as the upper bound of estimation error, there is

$$|\hat{f} - f| \leqslant \eta \tag{20}$$

*3.2. Adaptive Backstepping Control.* The first step of backstepping design is to define the tracking error as $e_1 = \phi_r - x_1$ and a virtual input as

$$\chi_1 = c_1 e_1 + \dot{\phi}_r \tag{21}$$

where $c_1$ is a positive constant.

Then define the angular velocity tracking error as

$$e_2 = \chi_1 - x_2 \tag{22}$$

and thus

$$\dot{e}_1 = \dot{\phi}_r - x_2 = -c_1 e_1 + e_2 \tag{23}$$

The derivative of the virtual input is

$$\dot{\chi}_1 = c_1\dot{e}_1 + \ddot{\phi}_r = -c_1^2 e_1 + c_1 e_2 + \ddot{\phi}_r \tag{24}$$

Design an adaptive controller as

$$\delta_z = \frac{c}{a_4}\hat{\gamma}\left(\dot{\chi}_1 - \hat{f} + \hat{\eta}\right)e_2 + \frac{c_2}{a_4}e_2 \tag{25}$$

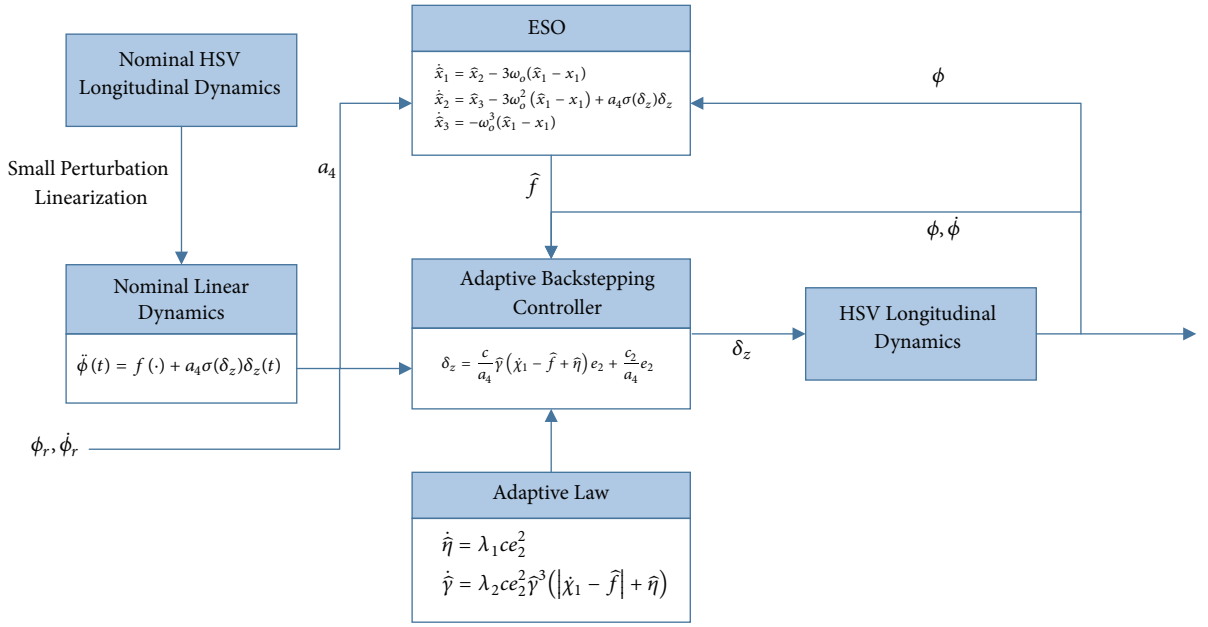


Figure 2: Block diagram of proposed ESO-based adaptive backstepping control structure for HSV system.

with adaption update laws

$$\begin{aligned}\dot{\hat{\eta}} &= \lambda_1 c e_2^2\\ \dot{\hat{\gamma}} &= \lambda_2 c e_2^2 \hat{\gamma}^3\left(\left|\dot{\chi}_1 - \hat{f}\right| + \hat{\eta}\right)\end{aligned} \tag{26}$$

where $c$, $c_2$, $\lambda_1$, and $\lambda_2$ are designed parameters.

The proposed ESO-based adaptive backstepping control structure for HSV system is shown in Figure 2.

*3.3. Stability Analysis.* The convergence of the tracking errors is established by Theorems 5 and 6.

**Theorem 5.** *For system (1) controlled by (25) and (26), where initial estimated values satisfy* $1/4cc_1 < \hat{\eta}(0) < \eta$, *the error* $e_2$ *converges into a small neighborhood of origin* $|e_2| < \epsilon = 1/(c - 1/4c_1\hat{\eta}(0))$ *within finite time* $t_\epsilon > 0$ *and is guaranteed to be uniformly ultimately bounded (UUB) for* $t \geqslant t_\varepsilon$.

*Proof.* Consider the Lyapunov function

$$V_1 = \frac{1}{2}e_1^2 + \frac{1}{2}e_2^2 + \frac{1}{2\lambda_1}\tilde{\eta}^2 + \frac{1}{2\lambda_2}\tilde{\gamma}^2 \tag{27}$$

where $\tilde{\eta} = \hat{\eta} - \eta$, $\tilde{\gamma} = \hat{\gamma}^{-1} - \gamma$, and $\gamma$ is a positive constant satisfying $0 < \gamma \leqslant \sigma(\delta_z) \leqslant 1$.

Considering the dynamics (7) and proposed control law (25), the derivative of $V_1$ can be derived as

$$\begin{aligned}\dot{V}_1 &= -c_1e_1^2 + e_1e_2 + e_2\dot{e}_2 + \frac{1}{\lambda_1}(\hat{\eta} - \eta)\dot{\hat{\eta}} - \frac{1}{\lambda_2}\left(\hat{\gamma}^{-1} - \gamma\right)\hat{\gamma}^{-1}\dot{\hat{\gamma}} = -c_1e_1^2 + e_1e_2 + \frac{1}{\lambda_1}(\hat{\eta} - \eta)\dot{\hat{\eta}} - \frac{1}{\lambda_2}\left(\hat{\gamma}^{-1} - \gamma\right)\hat{\gamma}^{-1}\dot{\hat{\gamma}} + e_2\left\{\dot{\chi}_1 - f\right.\\ &\left. - a_4\sigma(\delta_z)\left[\frac{c}{a_4}\hat{\gamma}\left(\dot{\chi}_1 - \hat{f} + \hat{\eta}\right)e_2 + \frac{c_2}{a_4}e_2\right]\right\}\\ &= -c_1e_1^2 + e_1e_2 + e_2(\dot{\chi}_1 - f) - ce_2^2\hat{\gamma}\sigma(\delta_z)\left(\dot{\chi}_1 - \hat{f} + \hat{\eta}\right) - c_2\sigma(\delta_z)e_2^2 + \frac{1}{\lambda_1}(\hat{\eta} - \eta)\dot{\hat{\eta}} - \frac{1}{\lambda_2}\left(\hat{\gamma}^{-1} - \gamma\right)\cdot\hat{\gamma}^{-1}\dot{\hat{\gamma}}\\ &= -c_1e_1^2 + e_1e_2 + e_2\left(\dot{\chi}_1 - \hat{f} + \hat{f} - f\right) - ce_2^2\hat{\gamma}\sigma(\delta_z)\left(\dot{\chi}_1 - \hat{f} + \hat{\eta}\right) - c_2\sigma(\delta_z)e_2^2 + \frac{1}{\lambda_1}(\hat{\eta} - \eta)\dot{\hat{\eta}} - \frac{1}{\lambda_2}\left(\hat{\gamma}^{-1} - \gamma\right)\hat{\gamma}^{-1}\dot{\hat{\gamma}}\end{aligned} \tag{28}$$

Let $\vartheta = |\dot{\chi}_1 - \hat{f}|$, then

$$\begin{aligned}\dot{V}_1 &\leqslant -c_1e_1^2 + |e_1e_2| + |e_2|(\vartheta + \eta) - ce_2^2\gamma\hat{\gamma}(\vartheta + \hat{\eta}) - c_2\gamma e_2^2 + \frac{1}{\lambda_1}(\hat{\eta} - \eta)\dot{\hat{\eta}} - \frac{1}{\lambda_2}\left(\hat{\gamma}^{-1} - \gamma\right)\hat{\gamma}^{-1}\dot{\hat{\gamma}}\end{aligned} \tag{29}$$

Substituting (26) into (29) yields

$$\begin{aligned}\dot{V}_1 &\leqslant -c_1e_1^2 + |e_1e_2| + |e_2|(\vartheta + \eta) - ce_2^2\gamma\hat{\gamma}(\vartheta + \hat{\eta}) - c_2\gamma e_2^2 + ce_2^2(\hat{\eta} - \eta) - ce^2(\vartheta + \hat{\eta})(1 - \gamma\hat{\gamma})\\ &= -c_1e_1^2 + |e_1e_2| + |e_2|(\vartheta + \eta) - c_2\gamma e_2^2 - ce_2^2(\vartheta + \eta)\end{aligned}$$

$$= -\left(\sqrt{c_1}\,|e_1| - \frac{1}{2\sqrt{c_1}}\,|e_2|\right)^2 + \frac{e_2^2}{4c_1} - c_2\gamma e_2^2 - ce_2^2(\vartheta+\eta) + |e_2|(\vartheta+\eta)$$
$$= -\left(\sqrt{c_1}\,|e_1| - \frac{1}{2\sqrt{c_1}}\,|e_2|\right)^2 - c_2\gamma e_2^2 - (\vartheta+\eta)\left[\left(c - \frac{1}{4c_1(\vartheta+\eta)}\right)e_2^2 - |e_2|\right] \tag{30}$$

Provided that $0 < \hat{\eta}(0) < \eta$, we obtain $0 < \hat{\eta}(0) < \vartheta + \eta$, that is,

$$\frac{1}{\vartheta+\eta} < \frac{1}{\hat{\eta}(0)} \tag{31}$$

Therefore,

$$\dot{V}_1 \leqslant -\left(\sqrt{c_1}\,|e_1| - \frac{1}{2\sqrt{c_1}}\,|e_2|\right)^2 - c_2\gamma e_2^2 - (\vartheta+\eta)\left[\left(c - \frac{1}{4c_1\hat{\eta}(0)}\right)e_2^2 - |e_2|\right] \tag{32}$$

Since $1/4cc_1 < \hat{\eta}(0)$, $\epsilon = 1/(c - 1/4c_1\hat{\eta}(0)) > 0$. If $|e_2| > \epsilon$,

$$\dot{V}_1 \leqslant -\left(\sqrt{c_1}\,|e_1| - \frac{1}{2\sqrt{c_1}}\,|e_2|\right)^2 - c_2\gamma e_2^2 \tag{33}$$

which means that $V_1$ is decreasing and bounded, and the error $e_2$ converges into a small neighborhood of origin; i.e., $|e_2| < \varepsilon$ within a finite time $t_\varepsilon > 0$. Even though the tracking error enters the region $|e_2| < \varepsilon$ within a finite time, it may move in and out since the nonnegativity cannot be guaranteed in the range. However, when it moves out, the Lyapunov function $V_1$ becomes negative again and the error is driven back to the region. Therefore, $e_2$ is guaranteed to be UUB for $t \geqslant t_{\varepsilon_z}$. □

**Theorem 6.** *Considering system (1) controlled by (25) and (26), the output tracking can be accomplished with virtual control input (21).*

*Proof.* To illustrate the reference state tracking, Lyapunov function is chosen as follows:

$$V_2 = \frac{1}{2}e_1^2 \tag{34}$$

The derivative of $V_2$ with (23) equals

$$\dot{V}_2 = -c_1e_1^2 + e_1e_2 \tag{35}$$

According to Theorem 5, it has been proved that $e_2$ is bounded. Thus, by selecting positive $c_1$ large enough, we obtain $\dot{V}_2 < 0$ when $V_2$ is out of a certain bounded region. Therefore, $e_1$ is also UUB by which $x_1$ tracking $\phi_r$ is guaranteed. Note that, from (35), it is clear that $V_2$ will not converge to zero due to the existence of $e_2$. It also implies that the state $x_1$ can only converge into a neighborhood of the origin and remain within it. □

Table 1: Control gains at feature points.

| Time(s) | $k_p$ | $k_d$ |
|---|---|---|
| 0 | 71.35 | 103.16 |
| 35 | 96.30 | 19.25 |
| 45 | 60.58 | 9.03 |
| 55 | 73.46 | 10.21 |
| 75 | 62.73 | 11.69 |
| 100 | 67.80 | 15.91 |
| 150 | 15.04 | 19.12 |

*Remark 7.* Small perturbation linearization is a typical engineering method for HSV attitude control and nominal values of parameters are usually used in the design process, which brings the problems of structural and parametric uncertainties. Applications indicate that ESO can estimate the total disturbance well even if $a_4$ is not calculated precisely. Thus the proposed method needs only a little model information and the adaptive law guarantees a smooth tracking performance within a wide flight envelope, which simplifies the designing process.

## 4. Simulation Results

In this section, simulation results for an HSV are provided to verify the feasibility and efficiency of the proposed control scheme. The reference trajectory used in the simulations is a typical trajectory of reentry segment. The longitudinal dynamics (1) are simulated as the real system, while the controller design procedure is based on the linearized model (3). The simulations are run for 150 seconds and at 100 samples per second. The controller gains are $c_1 = 10$, $c_2 = 20$, $c = 3$, $\lambda_1 = 0.1$, $\lambda_2 = 0.1$, and the ESO gains are tuned by bandwidth method with bandwidth $\omega_o = 5$. The initial value of adaptive gains are $\hat{\gamma}(0) = 0.1$, $\hat{\eta}(0) = 0.1$, and ones of estimations are $\hat{x}_1(0) = \hat{x}_2(0) = \hat{x}_3(0) = 0$. The deflection angle $\delta_z$ is bounded by $[-30^\circ, 30^\circ]$.

The control performance using an intelligent ADRC controller is also given to show the superiority of the proposed method. In the ADRC controller design, the control law is as follows:

$$\delta_z = k_p(\phi_r - \phi) + k_d(\dot{\phi}_r - \dot{\phi}) - \hat{f} \tag{36}$$

where $\hat{f}$ is the estimation of total disturbances by an ESO with the same bandwidth $\omega_o = 5$; control gains $k_p$, $k_d$ at several feature points are optimized by genetic algorithm (GA) according to the nominal linearized model and then interpolated, in order to achieve a smooth and quick tracking. The control gains at feature points are shown in Table 1.

To begin with, a set of comparative simulations for nominal longitudinal dynamics is studied, with no external disturbances and parametric uncertainties. Figure 3 shows the pitch angle tracking performance, and Figure 4 shows the tracking errors. The deflection angles are shown in Figure 5. Form the figures, it is indicated that both control methods can track the reference. Thanks to the excellent estimation ability of ESO to the internal "disturbance", the system can

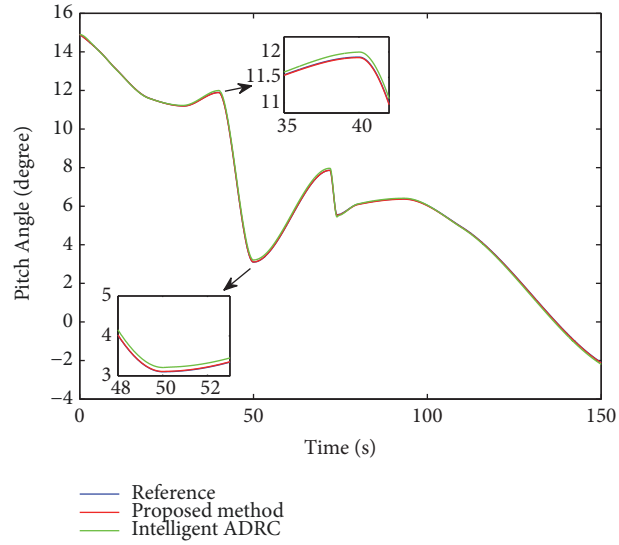


Figure 3: Pitch angle tracking performance for nominal longitudinal control system.

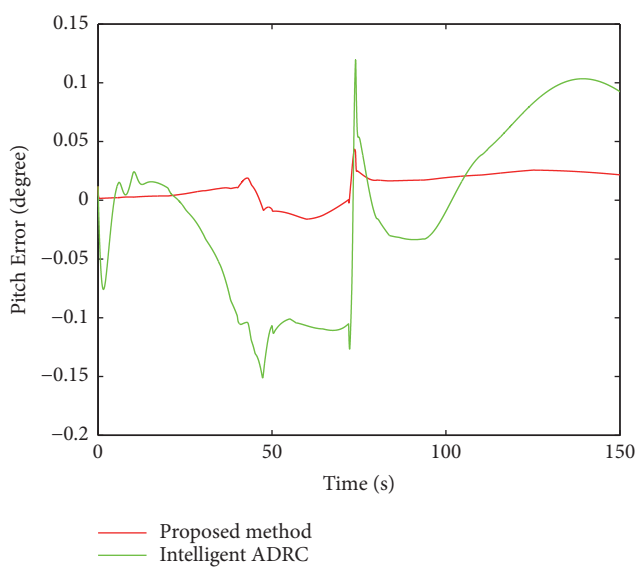


Figure 4: Pitch angle tracking error for nominal longitudinal control system.

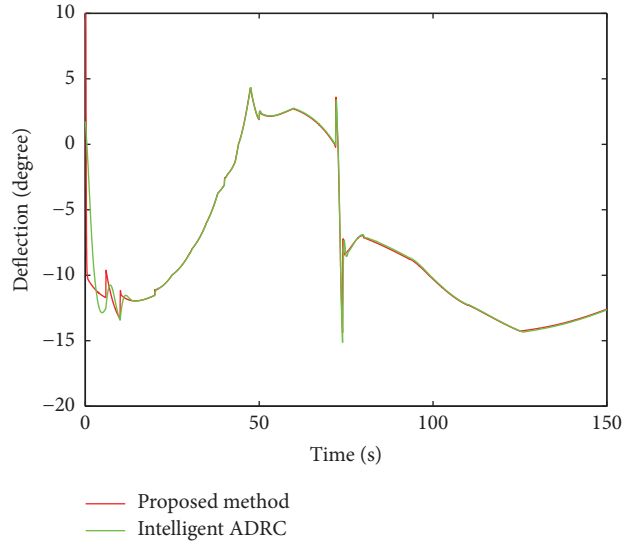


Figure 5: Deflection angle for nominal longitudinal control system.

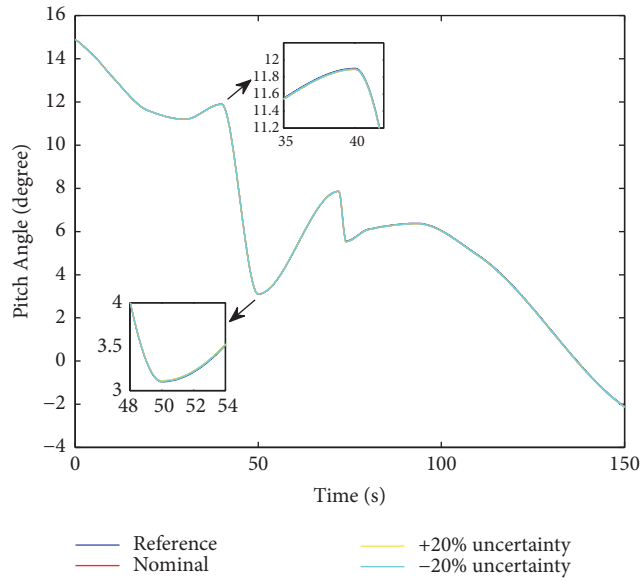


Figure 6: Pitch angle tracking performance using proposed control method subject to disturbance and parametric uncertainties.

be approximately transformed into a second-order integrator which is easier to be controlled.

It is easily seen from Figure 4 that the proposed controller tracks the reference more precisely. The ADRC controller can be regarded as a PD controller with compensation of disturbances. When the HSV works in a large flight envelop, especially when the reference pitch angle changes rapidly, the set of offline-tuned gains in ADRC may not perform well. Although the feature points will be selected more densely in practical applications, it may not reach the performance of a continuous adaptive method and the computational load will increase due to interpolation operations. Moreover, the parameter tuning procedure for traditional controllers like PID and ADRC is quite complex, while the proposed controller can be effective even in large envelop.

Then considering the existence of external disturbances and parametric uncertainties, another set of simulation is done. The simulations are done under sustained disturbance and abrupt reference changes. In the simulation, a sinusoidal wave disturbance is given as $M_{gz}(t) = 2 \times 10^3 \sin(0.5t)$ N·m, and uncertainty of ±20% in mass $m$ and moment of inertia $J_z$ is added to show the parameter robustness.

The tracking performance and tracking error of system using proposed control method are shown in Figures 6 and 7, while the ones using intelligent ADRC controller are shown in Figures 8 and 9. It can be inferred that both methods track the reference soon and remain stable in general due to the

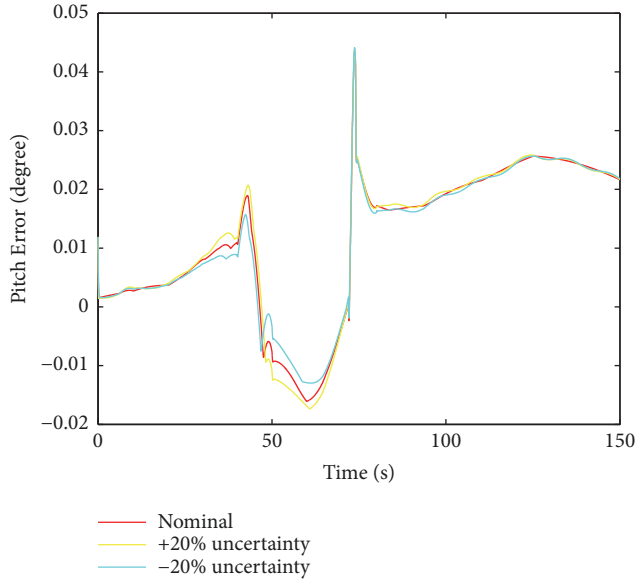


Figure 7: Pitch angle tracking error using proposed control method subject to disturbance and parametric uncertainties.

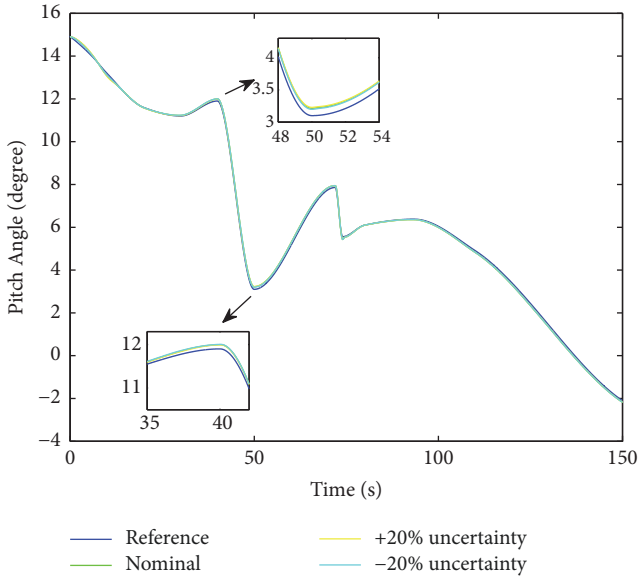


Figure 8: Pitch angle tracking performance using intelligent ADRC controller subject to disturbance and parametric uncertainties.

introduction of ESO. The time-varying disturbances, as well as parametric uncertainties and unmodeled dynamics, can be lumped together as the disturbances, which can be estimated by ESO and actively compensated for. However, the proposed method shows certain superiority in tracking error, since the controller gains are tuned adaptively. Also, the accuracy of disturbance estimation is ensured by setting the ESO gains large enough, but the existence of measurement noises adds a limit to observer gains in practical applications. Hence there will be a phase lag for estimation and the estimation error cannot be neglected. From this aspect, the adaptive method

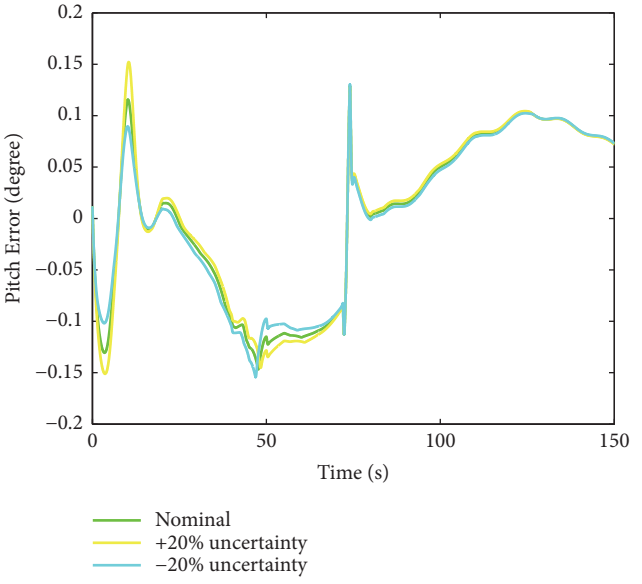


Figure 9: Pitch angle tracking error using intelligent ADRC controller subject to disturbance and parametric uncertainties.

estimates the upper bound $\eta$ of estimation error and can also handle it.

## 5. Conclusion

In this paper, the longitudinal control problem for HSVs subject to actuator saturation and disturbance is studied. Applying small perturbation assumption, the longitudinal dynamics can be considered as a second-order system at every trimming point, with total disturbance including unmodeled dynamics and parametric uncertainties. Then an ESO is constructed to estimate and compensate for the total disturbance actively, in order to decouple the system and improve the robustness. To deal with the large envelop and actuator saturation, an adaptive backstepping control scheme is designed to control the pitch angle. The presented method requires very little model information and the closed-loop convergence is proved. Finally, simulation results indicated a quick and smooth tracking performance and verified that the proposed method is effective. Further works may focus on the trajectory tracking control of HSV in 6 DoFs.

## Notation

$V$: Velocity of the HSV
$m$: Mass of the HSV
$g$: Gravitational constant
$J_z$: Pitch moment of inertia of the HSV
$\phi$: Pitch angle of the HSV
$\omega_z$: Pitch angular rate of the HSV
$X$: Drag force of the HSV
$Y$: Lift force of the HSV
$M_z$: Pitching moment of the HSV

$\theta$: Flight path angle of the HSV
$\alpha$: Angle of attack of the HSV
$\delta_z$: Deflection angle
$M_{gz}$: External disturbance moment.

## Data Availability

All the data used to support the findings of this study are available from the corresponding author upon request.

## Conflicts of Interest

The authors declare that they have no conflicts of interest.

## References


[1] Q. Wu, M. Sun, Z. Chen, Z. Yang, and Z. Wang, "Tuning of active disturbance rejection attitude controller for statically unstable launch vehicle," *Journal of Spacecraft and Rockets*, vol. 54, no. 6, pp. 1383–1389, 2017.

[2] J. S. Shamma and J. R. Cloutier, "Gain-scheduled missile autopilot design using linear parameter varying transformations," *Journal of Guidance, Control, and Dynamics*, vol. 16, no. 2, pp. 256–263, 1993.

[3] J. Yang, S. Li, C. Sun, and L. Guo, "Nonlinear-disturbance-observer-based robust flight control for airbreathing hypersonic vehicles," *IEEE Transactions on Aerospace and Electronic Systems*, vol. 49, no. 2, pp. 1263–1275, 2013.

[4] T. Çimen, "A generic approach to missile autopilot design using state-dependent nonlinear control," in *Proceedings of the 18th IFAC World Congress*, vol. 44 (1), pp. 9587–9600, Milano, Italy, September 2011.

[5] M. Sun, Z. Wang, and Z. Chen, "Practical solution to attitude control within wide envelope," *Aircraft Engineering and Aerospace Technology*, vol. 86, no. 2, pp. 117–128, 2014.

[6] Y. Xu, Z. Wang, and B. Gao, "Six-degree-of-freedom digital simulations for missile guidance and control," *Mathematical Problems in Engineering*, vol. 2015, Article ID 829473, 10 pages, 2015.

[7] D. Lin and J. Fan, "Missile autopilot design using backstepping approach," in *Proceedings of the 2009 Second International Conference on Computer and Electrical Engineering ICCEE'09*, vol. 1, pp. 238–241, IEEE, Dubai, UAE, December 2009.

[8] S. Lee, Y. Kim, G. Moon, and B.-E. Jun, "Missile autopilot design during boost phase using robust backstepping approch," in *Proceedings of the AIAA Guidance, Navigation, and Control Conference, 2015*, Kissimme, FL, USA, January 2015.

[9] J. Sun, S. Song, and G. Wu, "Tracking control of hypersonic vehicle considering input constraint," *Journal of Aerospace Engineering*, vol. 30, pp. 134–142, 2017.

[10] Z. Guo, J. Guo, and J. Zhou, "Adaptive attitude tracking control for hypersonic reentry vehicles via sliding mode-based coupling effect-triggered approach," *Journal of Aerospace Engineering*, vol. 78, pp. 228–240, 2018.

[11] A. B. Waseem, Y. Lin, and A. S. Kendrik, "Adaptive integral dynamic surface control of a hypersonic flight vehicle," *International Journal of Systems Science*, vol. 46, pp. 1–13, 2015.

[12] H. Xu, M. D. Mirmirani, and P. A. Ioannou, "Adaptive sliding mode control design for a hypersonic flight vehicle," *Journal of Guidance, Control, and Dynamics*, vol. 27, no. 5, pp. 829–838, 2004.

[13] J.-G. Sun, S.-M. Song, H.-T. Chen, and X.-H. Li, "Finite-time tracking control of hypersonic aircrafts with input saturation," *Proceedings of the Institution of Mechanical Engineers, Part G: Journal of Aerospace Engineering*, vol. 232, no. 7, pp. 1373–1389, 2018.

[14] C. Schumacher and P. P. Khargonekar, "Missile autopilot designs using H∞ control with gain scheduling and dynamic inversion," *Journal of Guidance, Control, and Dynamics*, vol. 21, no. 2, pp. 234–243, 1998.

[15] R. Rysdyk and A. J. Calise, "Robust nonlinear adaptive flight control for consistent handling qualities," *IEEE Transactions on Control Systems Technology*, vol. 13, no. 6, pp. 896–910, 2005.

[16] W. R. van Soest, Q. P. Chu, and J. A. Mulder, "Combined feedback linearization and constrained model predictive control for entry flight," *Journal of Guidance, Control, and Dynamics*, vol. 29, no. 2, pp. 427–434, 2006.

[17] H. An and Q. Wu, "Disturbance rejection dynamic inverse control of air-breathing hypersonic vehicles," *Acta Astronautica*, vol. 151, pp. 348–356, 2018.

[18] J. S. Brinker and K. A. Wise, "Stability and flying qualities robustness of a dynamic inversion aircraft control law," *Journal of Guidance, Control, and Dynamics*, vol. 19, no. 6, pp. 1270–1277, 1996.

[19] J. Reiner, G. J. Balas, and W. L. Garrard, "Robust dynamic inversion for control of highly maneuverable aircraft," *Journal of Guidance, Control, and Dynamics*, vol. 18, no. 1, pp. 18–24, 1995.

[20] G. Wu, X. Meng, and F. Wang, "Improved nonlinear dynamic inversion control for a flexible air-breathing hypersonic vehicle," *Aerospace Science and Technology*, vol. 78, pp. 734–743, 2018.

[21] C. Mu, Z. Ni, C. Sun, and H. He, "Air-breathing hypersonic vehicle tracking control based on adaptive dynamic programming," *IEEE Transactions on Neural Networks and Learning Systems*, vol. 28, no. 3, pp. 584–598, 2017.

[22] J. He, R. Qi, B. Jiang, and J. Qian, "Adaptive output feedback fault-tolerant control design for hypersonic flight vehicles," *Journal of The Franklin Institute*, vol. 352, no. 5, pp. 1811–1835, 2015.

[23] J. Q. Han, "From PID to active disturbance rejection control," *IEEE Transactions on Industrial Electronics*, vol. 56, no. 3, pp. 900–906, 2009.

[24] Z. Gao, "Scaling and bandwidth-parameterization based controller tuning," in *Proceedings of the American Control Conference*, vol. 6, pp. 4989–4996, Denver, Colo, USA, June 2003.

[25] Y. Huang, K. Xu, J. Han, and J. Lam, "Flight control design using extended state observer and non-smooth feedback in," in *Proceedings of the 40th IEEE Conference on Decision and Control*, vol. 1, pp. 223–228, IEEE, 2001.

[26] J. Tian, S. Zhang, Y. Zhang, and T. Li, "Active disturbance rejection control based robust output feedback autopilot design for airbreathing hypersonic vehicles," *ISA Transactions*, vol. 74, pp. 45–59, 2018.

[27] G. Zhang, L. Yang, J. Zhang, and C. Han, "Longitudinal attitude controller design for aircraft landing with disturbance using ADRC/LQR," in *Proceedings of the 2013 IEEE International Conference on Automation Science and Engineering, CASE 2013*, pp. 330–335, August 2013.

[28] B. Huang, A. Li, and B. Xu, "Adaptive fault tolerant control for hypersonic vehicle with external disturbance," *International Journal of Advanced Robotic Systems*, vol. 12, pp. 30–35, 2018.

[29] Q. Zheng, L. Q. Gao, and Z. Gao, "On stability analysis of active disturbance rejection control for nonlinear time-varying plants with unknown dynamics," in *Proceedings of the 46th IEEE Conference on Decision and Control (CDC '07)*, pp. 3501–3506, New Orleans, La, USA, December 2007.